



Sensor and Sensorless Speed Control of Doubly Fed Induction Generator Wind Turbines for Maximum Power Point Tracking

Fathy E. Abdel-Kader¹, Fahim A. Khalifa², Ahmed E. kalas³, Basem Elsaid^{2*}

ABSTRACT

Wind turbine output power can be maximized using maximum power point tracking (MPPT). By estimating wind speed, the MPPT can be achieved easily by adjusting the speed of DFIG based wind turbine through back-to-back converter. The grid side unity power factor can be simply achieved using PI controller on hybrid inverter. The aerodynamic power captured by wind turbine is the cosine function of pitch angle. In this paper, the pitch angle is kept zero, which is a valid assumption for lower to medium wind velocities. The machine side converter (MSC) is used to track the maximum power point for different wind speed. The grid side converter (GSC) uses a vector current controller to supply power at unity power factor to the grid. The simulations have been performed using MATLAB/SIMULINK. The effectiveness of proposed control methods validated.

Keywords—Maximum Power Point Tracking (MPPT), Doubly Fed Induction Generator (DFIG), Variable speed wind turbine (VSWT), Wind energy.

1. INTRODUCTION

Wind power is today's fastest growing renewable energy source. A wind turbine operates either at a fixed or variable speed rate [1]. Most of wind turbine manufacturers are developing new megawatt scale wind turbines based on variable-speed operation with pitch control using a doubly fed induction generator (DFIG) [2-4].

The variable speed wind turbine with DFIG and full-scale/fully controllable voltage source converters (VSCs) is considered to be a promising, but not yet very popular, wind turbine concept [3]. The wind turbines based on DFIG configuration have many advantages such as gearless construction [4], elimination of a dc excitation system [1-5].

Full controllability of the system for maximum wind power extraction and grid interface, and ease in accomplishing fault-ride through and grid support [6]. Therefore, the efficiency and reliability of a VSC-based DFIG wind turbine is assessed to be higher than that based DFIG [7]. Maximum power point tracking control in most of the conversion systems is implemented using wind speed data obtained from wind speed sensors [9-12]. However, accurate measurement of wind speed is not easy especially in case of large size wind turbines. Anemometer installed on the top of nacelle provides limited measurements of wind speed only at the hub height and cannot cover the whole span of large blades [13-15].

Due to the interaction between the rotor and the wind, anemometer, usually placed on nacelles, leads to inaccurate wind speed measurements in both upwind and downwind turbines. Therefore, Speed control of wind turbine based on sensor less algorithms has gained much interests due to its accuracy and simplicity in tracking the maximum power point during wind speed variations.

¹ Electrical Engineering Department Faculty of Engineering, Monofia University, Monofia, Egypt., E-mail:

fatkader2@yahoo.com

² Electrical Engineering, Faculty of Engineering, Suez Canal University, Ismailia, Egypt, E-mail:

Basem_elhady@yahoo.com

³ Electrical Engineering, Faculty of Engineering, Port Said University, Port Said, Egypt, E-mail:

kalas_14@yahoo.com

Doubly fed induction generator (DFIG) has been widely used for large-scale wind power generation systems due to its advantages, such as variable speed operation, controllable power factor and improved system efficiency [3]. The amount of energy extracted from the wind depends not only on the incident wind speed, but also on the control system applied on the wind energy conversion system (WECS). Typically, maximum wind power extraction is accomplished by using fully controlled variable speed wind turbine generators. The rotational speed of wind turbine hub is adjusted according to the incident wind speed to track the maximum wind power trajectory [1], [4]. In this paper, maximum power point tracking for wind turbine based DFIG has been achieved by wind velocity estimation technique. Estimation of the wind velocity was made considering the relation between the system efficiency and the injected power to the grid. A full scale power converter based five-phase has been used. The dc-link, connecting the back-to-back converters, allow fully decoupled control of DFIG from the grid side. The MPPT has been achieved by controlling the DFIG speed at the generator side, whereas the grid side converter has been controlled to achieve unity power factor at the grid side. The effectiveness of the proposed control technique in addition to the efficient operation of the wind turbine system based on DFIG has been verified using Matlab/Simulink.

2. SYSTEM MODELING

Wind Energy Conversion System (WECS) converts kinetic energy of the wind to mechanical energy by means of wind turbine rotor blades then the generator converts the mechanical power to electrical power that is being fed to the grid through power electronic converters. The WECS under study, described in Fig. 1, consists of two main parts: a) Mechanical parts: include the aerodynamic system with the rotor blades. b) Electrical parts: comprised of the DFIG and the back-to-back converter set [2], and [5-6].

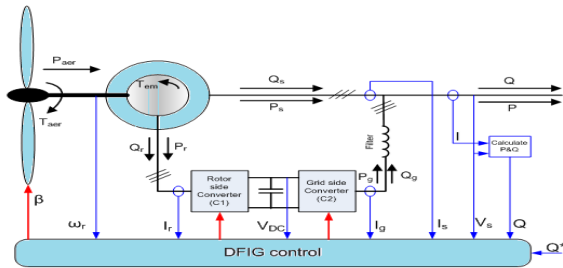


Fig.1: Power flow and control diagram of DFIG [5].

A. Mechanical Part Representation

The aerodynamic rotor is responsible for converting wind power incident on turbine rotor blades which rotate with swept area ($A = \pi R^2$), to mechanical power form. The mechanical power is given as follows:

$$P_m = \frac{1}{2} C_p \rho \pi R^2 V_{wind}^3 \quad (1)$$

Where; ρ is the air density (Kg/m^3), R is the blade length (m), V_{wind} is wind speed (m/s) and C_p is the power coefficient. The value of C_p is dependent on the tip speed ratio (λ) and the blades pitch angle (β). The blades pitch angle is adjusted by the embedded pitch controllers and depends on the type and operating condition of the wind turbine. The mathematical expression of C_p is given by [1], [5] and [7] as;

$$C_p = c_1 \left(\frac{c_2}{\lambda_i} - c_3 \beta - c_4 \right) e^{-\frac{c_5}{\lambda_i}} + c_6 \lambda \quad (2)$$

The parameters λ_i and $c_1 - c_6$ are defined in the Appendix [6]. The tip speed ratio is given as follows:

$$\lambda = \frac{\omega_t R}{V_{wind}} \quad (3)$$

where: ω_t (rad/s) is the rotational speed of the turbine shaft. The mechanical input torque, T_m , is given as follows:

$$T_m = \frac{P_m}{\omega_t} \quad (4)$$

Fig.2 shows the relation between C_p and λ for different pitch angles. The maximum value of the power coefficient, $C_{p_max} \approx 0.48$, is obtained at $\beta = 0^\circ$ and $\lambda = \lambda_{opt} \approx 8.1$. Fig.3 describes the wind turbine output power characteristics. Based on Fig.3, for any particular wind speed, there is optimum rotational speed, which gives the maximum power capturing.

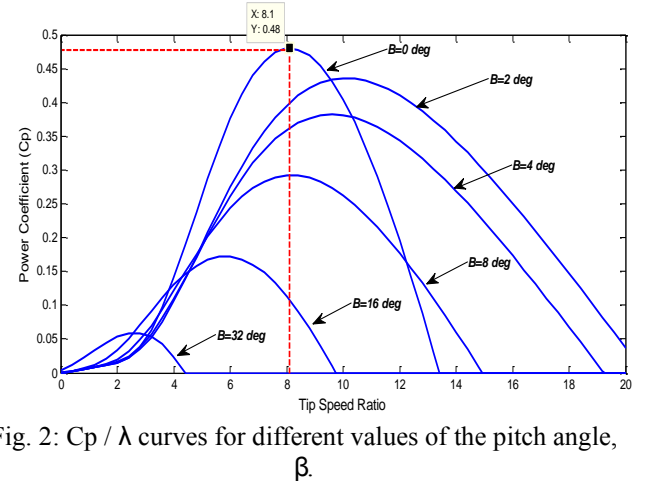


Fig. 2: C_p / λ curves for different values of the pitch angle, β .

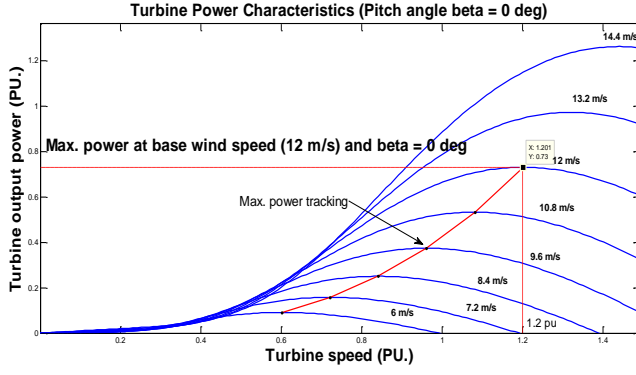


Fig. 3: The power characteristics of the wind turbine used.

B. Electrical Part Representation

As shown in Fig. 1, variable speed wind turbine DFIG is connected directly to the utility grid through the stator. The rotor is connected via a back-to-back set of converters. The first converter, known as the rotor side converter, is connected to the rotor windings of the DFIG. While the other one is known as grid side converter and is connected to the grid at the PCC via ac filter. The dc terminals of the two converters are collected together with shunt dc capacitor. DFIG model with detailed description along with the control schemes of the interfacing converters are presented in MATLAB/SIMULINK environment as in [3] and [5].

B.1 Modeling of DFIG

The mathematical model of the DFIG presented in this paper uses the d-q synchronous reference frame illustrated in Fig. 4.

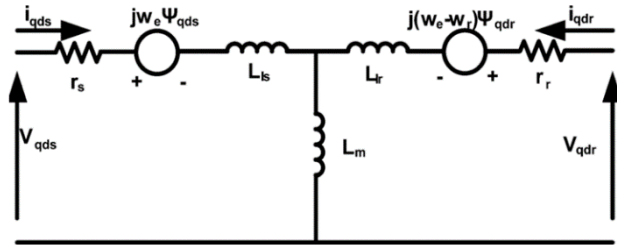


Fig. 4: Doubly fed induction generator model.

The d-q synchronous reference frame equations of the stator and rotor flux are written as [3], [8] and [9]:

$$V_{qs} = R_s i_{qs} + \frac{d}{dt} \varphi_{qs} + \omega \varphi_{ds} \quad (5)$$

$$V_{ds} = R_s i_{ds} + \frac{d}{dt} \varphi_{ds} - \omega \varphi_{qs} \quad (6)$$

$$V'_{qr} = R'_r i'_{qr} + \frac{d}{dt} \varphi'_{qr} + (\omega - \omega_r) \varphi'_{dr} \quad (7)$$

$$V'_{dr} = R'_r i'_{dr} + \frac{d}{dt} \varphi'_{dr} - (\omega - \omega_r) \varphi'_{qr} \quad (8)$$

$$\varphi_{qs} = L_s i_{qs} + L_m i'_{qr} \quad (9)$$

$$\varphi_{ds} = L_s i_{ds} + L_m i'_{dr} \quad (10)$$

$$\varphi'_{qr} = L'_r i'_{qr} + L_m i_{qs} \quad (11)$$

$$\varphi'_{dr} = L'_r i'_{dr} + L_m i_{ds} \quad (12)$$

$$L_s = L_{ls} + L_m \quad (13)$$

$$L'_r = L'_{lr} + L_m \quad (14)$$

The active and reactive power equations at the stator and rotor windings are written as:

$$P_s = V_{ds} i_{ds} + V_{qs} i_{qs} \quad (15)$$

$$Q_s = V_{qs} i_{ds} - V_{ds} i_{qs} \quad (16)$$

$$P_r = V_{qr} i_{dr} + V_{qr} i_{qr} \quad (17)$$

$$Q_r = V_{dr} i_{dr} - V_{dr} i_{qr} \quad (18)$$

The electromagnetic torque is expressed as:

$$T_{em} = \frac{3}{2} * \frac{P}{2} (\varphi_{ds} i_{qs} - \varphi_{qs} i_{ds}) \quad (19)$$

Where: v_{ds}, v_{qs} : Stator Voltages in D-Q axis reference Frame, v_{dr}, v_{qr} : Rotor Voltages in D-Q axis reference Frame, i_{ds}, i_{qs} : Stator Currents in D-Q axis reference Frame, i_{dr}, i_{qr} : Rotor Currents in D-Q axis reference Frame, ϕ_{ds}, ϕ_{qs} : Stator Flux Linkages in D-Q axis reference Frame, ϕ_{dr}, ϕ_{qr} : Rotor Flux Linkages In D-Q Axis Reference Frame, P_s, Q_s : Stator Active, Reactive Power, P_r, Q_r : Rotor Active, Reactive Power, R_s, R_r : Stator and Rotor Resistance per phase, ω_e, ω_r : Supply and Rotor Flux Angle, L_s, L_r : Stator and Rotor Inductance, L_{ls}, L_{lr}, L_m : Stator, Rotor Leakage Inductance, and Magnetizing

Inductance, and T_e : Electromagnetic Torque.

The control of doubly fed induction generator with wind turbine is necessary and unavoidable. The control system maintains magnitudes of the generator, such as torque, active and reactive power, related to the grid side converter. The reactive power and the DC bus voltage close to their optimum values, for proper and effective energy generation [15-20]. The Control schemes of DFIG based wind turbine will be described in details in the following sections.

3. CONTROL OF THE ROTOR SIDE CONVERTER

The control strategy for the rotor side converter is shown in Fig. 5. The active power flow is controlled through i_{dr} and the reactive power flow is controlled through i_{qr} . The standard voltage oriented vector control strategy is used for the rotor side converter to implement control action. Here the real axis of the stator voltage is chosen as the d-

axis [11]. The actual speed of the turbine ω_r is measured and the corresponding mechanical power of the tracking characteristic is used as the reference power for the power control loop. The actual electrical output power, measured at the grid terminals of the wind turbine is added to the total power losses (mechanical and electrical) and is compared with the reference power obtained from the tracking characteristic.

A Proportional-Integral (PI) regulator is used to reduce the power error to zero. The output of this regulator is the reference rotor current I_{dr_ref} that must be injected in the rotor by the converter. This is the current component that produces the electromagnetic torque T_{em} . The actual I_{dr} component is compared to I_{dr_ref} and the error is reduced to zero by a current regulator (PI). The output of this current controller is the voltage V_{dr} generated by control of the rotor side converter. The current regulator is assisted by feed forward terms which predict V_{dr} . I_{q_ref} is set zero to obtain zero reactive power as shown in Fig.5 [17-22].

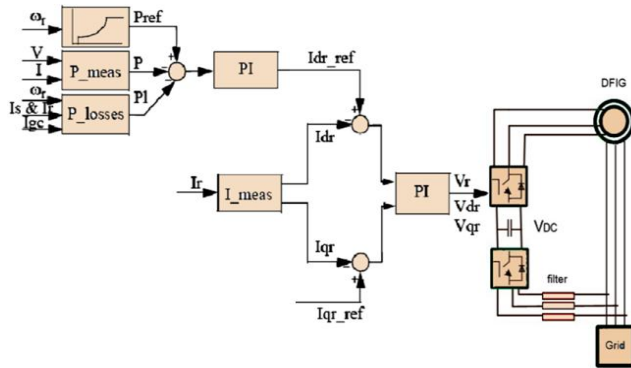


Fig.5: Vector control structure of rotor side converter.

4. CONTROL OF THE GRID SIDE CONVERTER

The main objective of the grid side converter is to maintain the DC - link voltage constant for the necessary action. For the grid-side controller, the d-axis of the rotating reference frame used for d-q transformation is aligned with the positive-sequence of grid voltage. The control system is shown in Fig.6. This controller consists of; (1) Measurement system which measures the d and q components of AC currents to be controlled as well as the DC voltage V_{dc} , (2) Outer regulation loop consisting of a DC voltage regulator. The output of the DC voltage regulator is the reference current I_{dgc_ref} for the current regulator (I_{dgc} = current in phase with grid voltage which controls active power flow). (3) An inner current regulation loop consisting of a current regulator. The current regulatory controls the magnitude and phase of the voltage generated by converter from the I_{dgc_ref} produced by the DC voltage regulator and specified I_{q_ref} [10], and [22-24]. The DC link voltage can be expressed as:

$$C \frac{dV_{dc}}{dt} = \frac{3}{4} m i_{gd} - i_{rdc} \quad (20)$$

Where i_{gd} is the d-axis current flowing between the grid and the grid side converter, i_{rdc} is the rotor side DC current, C is the DC link capacitance; m is the PWM modulation index of the grid side converter. The reactive power flow into the grid Q_g is calculated as

$$Q_g = \frac{3}{2} (V_g i_{gq}) \quad (21)$$

Where V_g is the magnitude of the grid phase voltage, i_{gq} is the q-axis current flowing between the grid and the grid side converter. From eq. (20) and eq.(21), the DC link voltage and the reactive power flow into the grid can be controlled via i_{gq} .

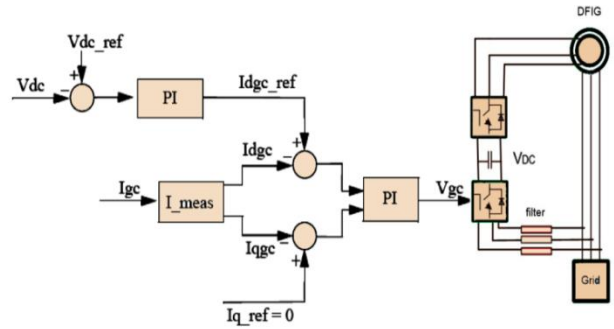


Fig.6: Vector control structure of Grid side Converter.

4.1. Optimal torque (OT) control (sensor)

As mentioned previously, maintaining the operation of the system at λ_{opt} ensures the conversion of available wind energy into mechanical form. It can be observed from the block diagram in Fig.7 [15] that the principle of this method is to adjust the DFIG torque according to a maximum power reference torque of the wind turbine at a given wind speed. For the turbine power to be determined as a function of ω_m , the following equation will be adopted in order to obtain the wind speed [20-26]:

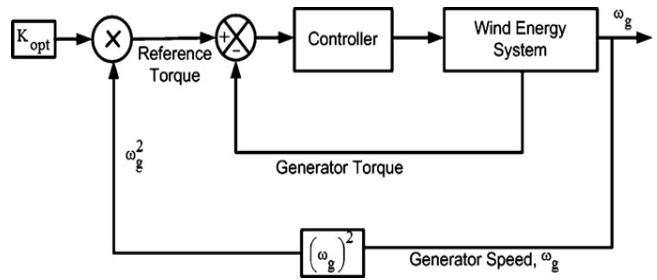


Fig.7. The block diagram of optimal torque control for MPPT control.

Using eq.(1) & (3), the output optimum power wind turbine can be written as

$$P_{m_opt} = 0.5\rho AC_p \left(\frac{\omega_{m_opt} R}{\lambda_{opt}} \right)^3 \quad (22)$$

Where

$$K_{opt} = 0.5\rho AC_p \left(\frac{R}{\lambda_{opt}} \right)^3 \quad (23)$$

$$P_{m_opt} = K_{opt} (\omega_{m_opt})^3 \quad (24)$$

Consider that $P_m = T_m \cdot \omega_m$

$$T_{m_opt} = K_{opt} (\omega_{m_opt})^2 \quad (25)$$

Fig.3 indicates the mechanical power generated by the turbine as a function of rotor speed for different wind speeds. The maximum power extraction within the allowable range can be achieved if the controller can properly follow the optimum curve with variation of wind speed.

4.2. Sensorless Wind Speed Estimation Technique

From eq.(1),(3),and (27) wind speed can be estimated if the value of mechanical power and power coefficient which is a function in rotor speed and wind speed are known. Eq. (28) governs the estimated wind speed. Fig.8 shows representation of eq.(29).

$$\zeta = \frac{p_m}{p_e} \quad (26)$$

$$\frac{p_e}{\xi} = \frac{1}{2} \rho A C_p V_w^3 \quad (27)$$

$$V_w = \sqrt[3]{\frac{P_e}{\xi * C_p * K_{opt}}} \quad (28)$$

$$V_w = \left(\frac{P_e}{0.5\rho AC_p \eta} \right)^{\frac{1}{3}} \quad (29)$$

To estimate the wind speed from eq.(26), the efficiency η of the DFIG is assumed to be equal to 92% and losses converter are neglected

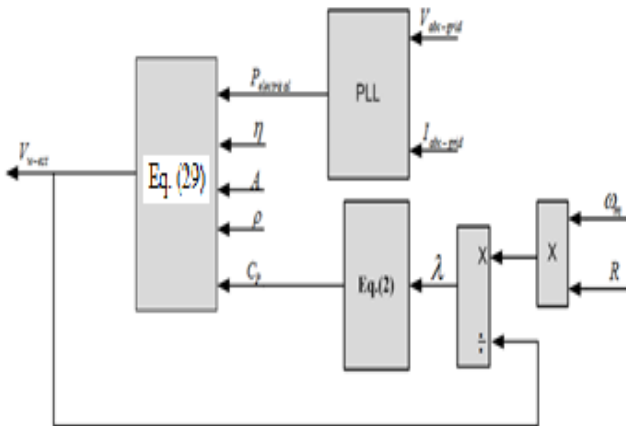


Fig.8 Estimated wind speed block diagram

5. Simulation Results and discussion

The parameters of the system under study are given in appendix A. MATLAB/SIMULINK software is used to perform the simulation using power system block sets with a simulation time of 1.5 seconds. The proposed control scheme for DFIG based variable speed WECS is simulated using MATLAB/Simulink under different cases for wind speed variations.

Case study no.1:

Fig.9 shows the wind speed profile, which varies up and down with smooth ramp rates, with an average value of 11.05 m/s. Further wind speed is estimated.

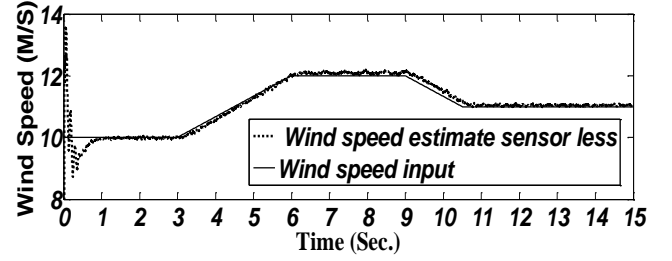
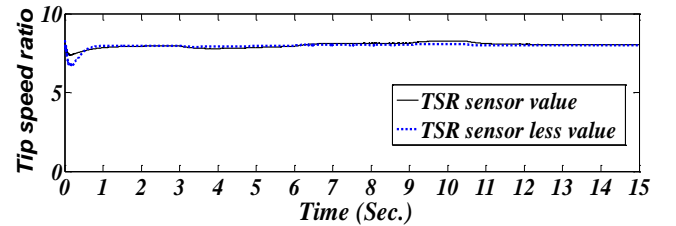
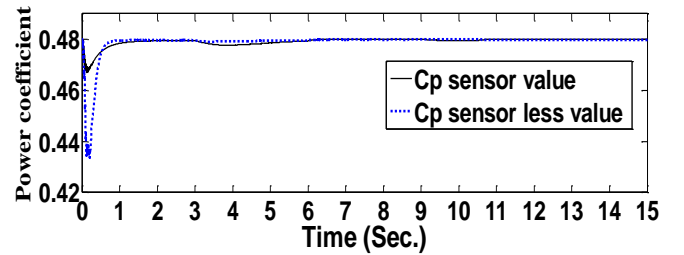


Fig.9 Ramp change in actual wind speed & estimated wind speed in m/s.

Results show that sensorless control has better performance than sensor-type control. As seen from Fig.10, the maximum power capture is achieved, hence the tip speed ratio λ achieves the optimality ($\lambda=8.1$) and C_p is constant at its maximum value ($C_p=0.48$).



(a)



(b)

Fig.10 (a) Tip speed ratio λ (b) power coefficient C_p .

Fig.11 and Fig.12 show the impact of the control system on the rotational speeds of the generator, the mechanical torque curve, and the same determination-oriented electrical torque result of

lack of gear box, which clearly shows that it takes the same wind speed profile except at sudden change where the moment of inertia appeared.

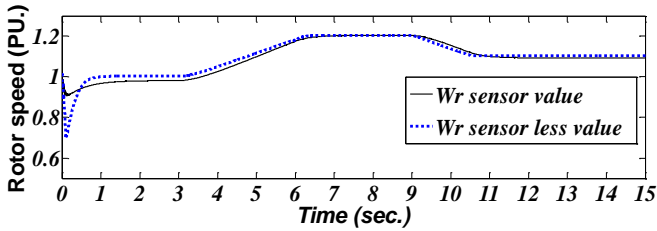


Fig.11 Rotational speed of the generator.

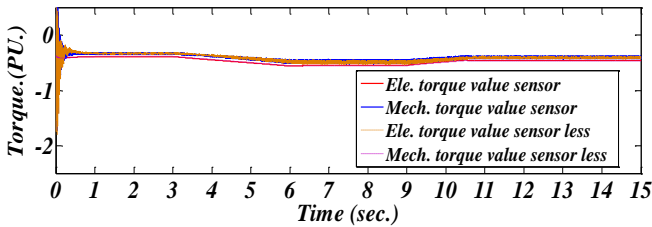
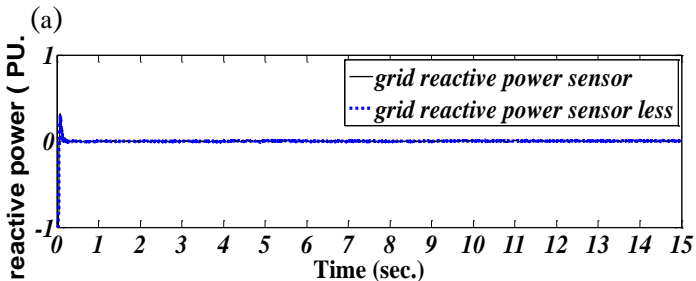
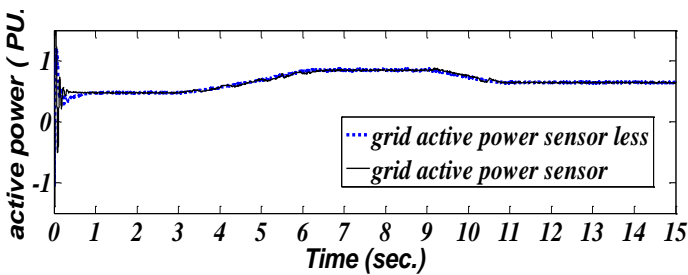


Fig.12 Mechanical & electrical torque of the generator.

Fig.13 (a) and (b) illustrate the grid active and reactive power respectively. As shown in Fig.13(a), the control system used achieve that power injected to the grid is varied with wind speed variation and the reactive power injected to the grid is zero (i.e. unity power factor) as shown in Fig.13 (b).



(b)

Fig.13 (a) Grid active power. (b) Grid reactive power.

From Fig.14, the Dc-link voltage ripple is reduced ($V_{DC} \sim V_{ref}$ (1200v)) and almost constant over the all period of simulation time.

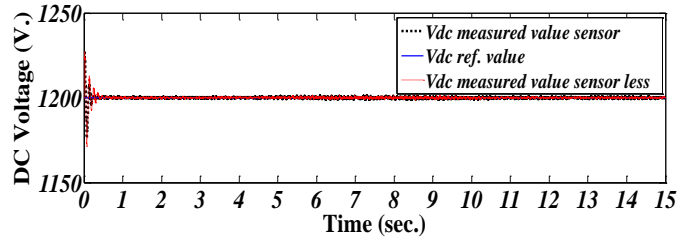


Fig.14 DC link voltage in Volt.

Case study no.2

The wind speed profile varies randomly with mean value of 10 m/s and 20% turbulence intensity according to wind model. Further wind speed is estimated of Wind Turbine Block set in Matlab/Simulink [27] as shown in Fig.15.

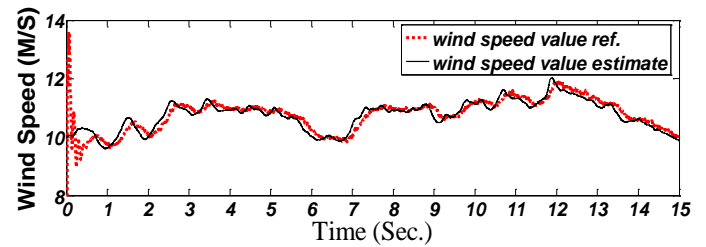


Fig.15 Random change in wind speed & wind speed estimate in m/s.

Fig.16, and Fig.17 show the impact of control system on rotational speeds of generator, mechanical torques curve with same determination oriented electrical torque result of lack of gear box, which clearly shows that it takes the same wind speed variation.

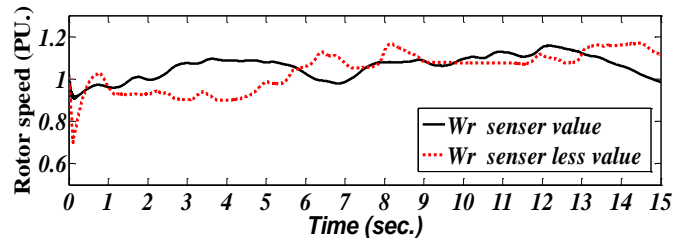


Fig.16 Rotational speed of the generator.

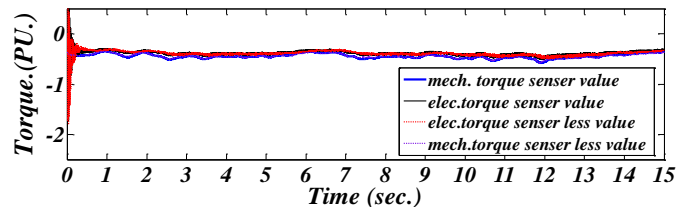
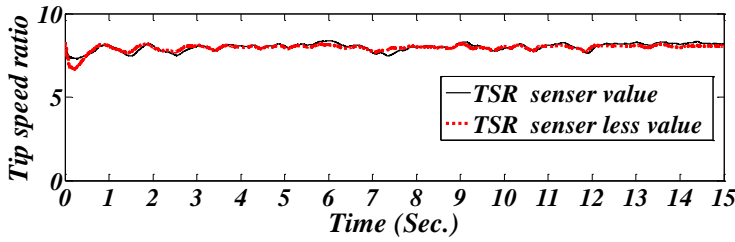


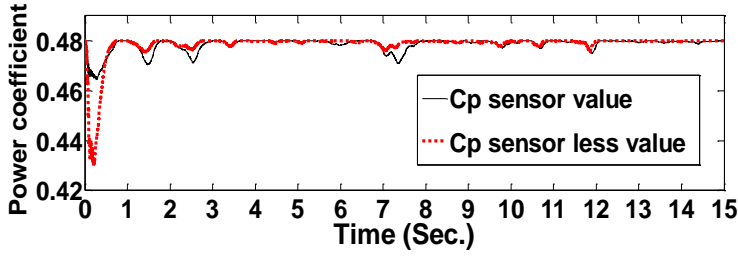
Fig.17 Mechanical & Ele. Torque of the generator.

As shown in Fig.18 (a) and (b) respectively the control scheme of the rotor side converter gives better performance using sensor, and sensor less MPPT control scheme for DFIG. The maximum power capture is achieved, hence the tip speed ratio λ achieve the

optimality($\lambda=8.1$) and C_p is constant at maximum value ($C_p=0.48$).



(a)



(b)

Fig.18 (a) Tip speed ratio λ (b) power coefficient C_p .

I_d and I_q are shown in Fig.19, I_d varied with wind speed and $I_q=0$.

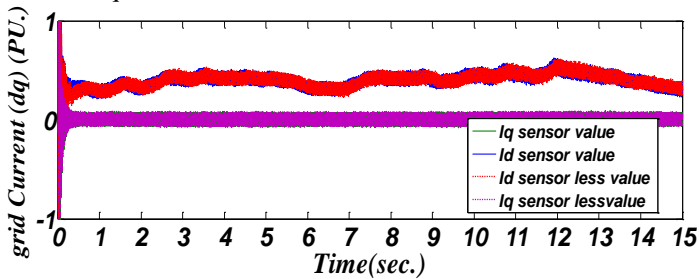
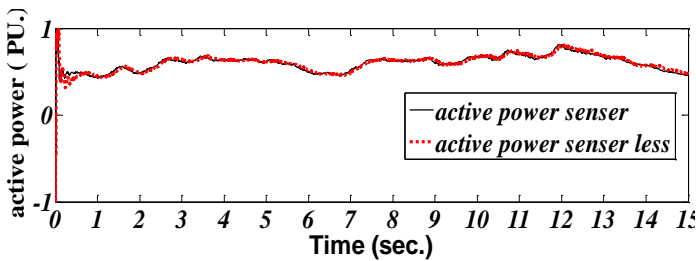
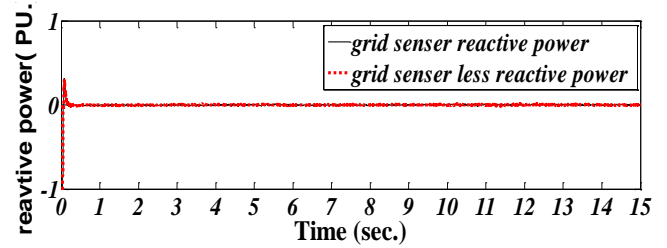


Fig.19 grid Current I_d and I_q

In Fig.20 (a) and (b) the grid active power and grid reactive power is discussed respectively where the reactive power is nearly zero, hence unity power factor is achieved. control system used achieve that power injected to the grid is varied with wind speed variation and the reactive power injected to the grid is zero.



(a)



(b)

Fig.20 (a) Grid active power in pu (b) Grid reactive power.

The DC link voltage is nearby constant ($V_{DC} \sim V_{ref}$ (1200v)) over the all period of simulation time by using grid side converter as seen in Fig.21.

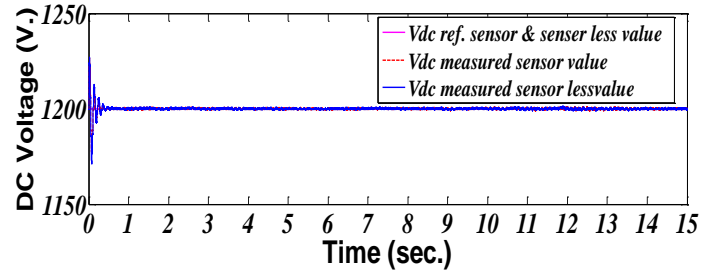


Fig.21 DC link voltage in Volt.

6.CONCLUSION:

This paper has presented a comprehensive modeling of direct driven DFIG based grid-connected wind turbines along with control schemes of the interfacing converters. Grid power has been achieved based on the injected wind velocity estimation in addition to the system efficiency.

Three-phase interface power converter based on back-to-back common dc-link converter has been used to achieve the system objectives. The generator side converter based three-phase has been used to achieve maximum power operation point at each wind speed. The grid side converter based three-phase has been used to inject sinusoidal current in-phase with the grid voltage in addition to controlling the common dc-link capacitor voltage. Vector current controller has been employed on the grid side VSI to obtain unity power factor. Simulation results prove that the proposed control scheme has a great capability to obtain unity power factor at the grid side and to achieve sensorless maximum power point tracking of wind turbine based on DFIG during wind speed variation.

Results show that sensorless control gives better performance than sensor type control. Sensorless control manage to trace the variations in wind speed.

7. REFERENCES

- [1] Committee on Environmental Impacts of Wind Energy Projects, "Environmental Impacts of Wind Energy Projects", Washington, The National Academies Press, 2007.
- [2] Report of New and Renewable Energy Authority, available on line at <http://www.nrea.gov.eg> last access 20 Oct 2014.
- [3] Thongam, Jogendra Singh, and Mohand Ouhrouche. "MPPT Control Methods in Wind Energy Conversion Systems", available online at <http://www.intechopen.com> last access 22 Oct 2014
- [4] Acharya, Parash, "Small Scale Maximum Power Point Tracking Power Converter for Developing Country Application", Master of Engineering, University of Canterbury, Christchurch, New Zealand. (2013).
- [5] Ali H. Kasem Alaboudy, Ahmed A. Daoud, Sobhy S. Desouky, and Ahmed A. Salem, "Converter Controls and Flicker Study of PMSG- Based Grid Connected Wind Turbines", Ain Shams Engineering Journal, Elsevier, vol. 4, issue 1, pp. 75-91, Mar. 2013.
- [6] M. Chinchilia, S. Arnaltes, and J. Burgos, "Control of Permanent- Magnet Generator Applied to Variable- Speed Wind -Energy Systems Connected to the Grid," IEEE Trans. Energy Conversion, vol. 21, no.1, Mar. 2006
- [7] S. Muller., M. Deicke, and R. W. De Doncker, "Doubly fed induction generator systems for wind turbines," IEEE Ind. Appl. Mag., vol. 8, no.3,pp. 26-33, May/June. 2002.
- [8] K.Tan, and S.Islam, "Optimum Control Strategies in Energy Conversion of PMSG Wind Turbine System without Mechanical Sensors," IEEE Trans. Energy Conversion, vol.19, no.2, Jun. 2004.
- [9] Ahmed A. Daoud, Sobhy S. Dessouky, and Ahmed A. Salem, "Control Scheme of PMSG Based Wind Turbine for Utility Network Connection," in 10th IEEE Proc., Rome, Italy, May 8-10, 2011.
- [10] Abdullah, M. A., A. H. M. Yatim, C. W. Tan, and R. Saidur, "A review of maximum power point tracking algorithms for wind energy systems" Renewable and Sustainable Energy Reviews 16, no. 5 (2012): 3220-3227.
- [11] M.H. Elfar, "Maximum Power Tracking Algorithm for Wind Energy Systems Based on Artificial Intelligence", PHD theses, Suez Canal University, 2010.
- [12] G. Podder, A. Joseph, and A. Unnikrishnan, "Sensorless Variable-Speed Controller for Existing Fixed-Speed Wind Power Generator with Unity-Power-Factor Operation", IEEE Trans. Ind. Electron., Vol. 50, No. 5, pp.1007-1015, Oct. 2003.
- [13] Francoise Mei and Bikash Pal, "Modal Analysis of Grid-Connected Doubly Fed Induction Generators", IEEE Transactions on Energy Conversion, Vol. 22, No.3, pp. 728-736, September 2007.
- [14] Xin Jing, "Modeling And Control Of A Doubly Fed Induction Generators for Wind Turbine Generator Systems", Master theses, Marquette University, December 2012.
- [15] Alireza Abbaszadeh, Saeed Lesan and Vahid Mortezaipoor, "Transient Response of Doubly Fed Induction Generator Under Voltage Sag Using an Accurate Model", 2009 IEEE PES/IAS Conference on Sustainable Alternative Energy (SAE), pp. 1-6, September 2009.
- [16] Abdullah MA, Yatim AHM, Tan CW. "A study of maximum power point tracking algorithms for wind energy system", 2011 IEEE, first conference on clean energy and technology (CET). 2011. p. 321-6.
- [17] R. Data and V. Ranganathan, "A Method of Tracking the Peak Power Points for a Variable Speed Wind Energy Conversion System", IEEE Trans. Energy Conversion, Vol. 18, No.1 pp.163-168, Mar.2003.
- [18] Q. Wang, L. Chang, "An Intelligent Maximum Power Extraction Algorithm for Inverter-Based Variable Speed Wind Turbine System," IEEE Trans. Power Electronics, Vol. 19, No. 5, pp.1242-1249, Sept. 2004.
- [19] W.M.Lin, C.M. Hong, and F.S.Cheng, "Fuzzy neural network output maximization control for sensor less wind energy conversion system," Energy, vol. 35, no. 2, pp. 592-601, Feb. 2010.
- [20] J.S.Thongam,P.Bouchard, H. Ezzaidi and M.Ouhrouche, "Artificial Neural Network Based Maximum Power Point Tracking Control for Variable Speed Wind Energy Conversion Systems," in proc. of IEEE MSC2009, July 8-10,2009.
- [21]M.M.Hussien, M.Orabi,Mahrous.E.Ahmed, and M.A.Elwahab, "Simple direct sensorless control of permanent magnet synchronous generator wind turbine," in Proc. of 14th international Middle East Power System Conf. (MEPCON'10), Cairo university, Egypt., Dec.19-21,2010.
- [22] Anca D. Hansen, Florin Iov, Poul Sørensen, Frede Blaabjerg, "Overall control strategy of variable speed doubly-fed induction generator wind turbine," Nordic Wind Power Conference, 1-2 Mar. 2004.
- [23] F. Mei and B. Pal, "Modal Analysis of Grid-Connected Doubly Fed Induction Generators", IEEE Trans. on Energy Conversion, Vol. 22, No. 3, September 2007, pp. 728-736.
- [24] L. Xu, and Y. Wang, "Dynamic Modeling and Control of DFIG -Based Wind Turbines Under Unbalanced Network Conditions", IEEE Transactions on Power Systems, Vol. 22, No.1, February 2007, pp. 314-323.
- [25] A. H. Kasem Alaboudy, "Power conditioning and performance enhancement of wind based distributed generation," PhD thesis, Minia University,

Egypt, 2009.

[26] Ion Boldea, “Variable speed generators” (Electric power engineering series). Publ.CRC 2005.

[27] F. Iov, A. D. Hansen, P. Sorensen, and F. Blaabjerg, “Wind Turbine Blackest in Matlab/Simulink, Research Project”, Institute of Energy Technology, Alborg University, Mar. 2004.

Appendix A. Specification of wind turbine

The coefficients C_1 to C_6	$C_1 = 0.5167$	116	$C_3 = 0.4$
	$C_2 = 116$		$C_3 = 0.4$
	$C_4 = 5$	$C_5 = 21$	$C_6 = 0.0068$
Wind turbine blade radius	$R = 1.8m$		
Air density	$\rho = 1.25kg/m^3$		
Optimal tip speed ratio	$\lambda_{opti} = 8.1$		
Maximum power	$C_{p-max} = 0.48$		
Coefficient			

Appendix B. Parameter of IG

Stator phase resistance (R_s)	0.023PU
Stator direct inductance (L_d)	0.18 PU
Rotor phase resistance (R_r)	0.016 PU
Rotor direct inductance (L_d)	0.16 PU
No. of pole pairs (P)	3 pair pole
Inertia of the whole system (J)	0.0095 N.m
Friction factor (B)	0.05479 PU

Appendix C. DC bus and grid parameters

dc-link voltage	$V_{dc} = 1200$
Capacitor of the dc-link	$C = 6\mu F$
Grid frequency	$F = 50hz$
Grid resistance	$R_g = 0.02\Omega$
Grid inductance	$L_g = 0.05mH$

Appendix d . PI parameters

Rotor .side current loop:	K_p	0.3
	K_i	8
Grid side current loop:-	K_p	0.44
	K_i	0.008
Dc-link loop:-	K_p	4
	K_i	400

Appendix D. MATLAB/SIMULINK

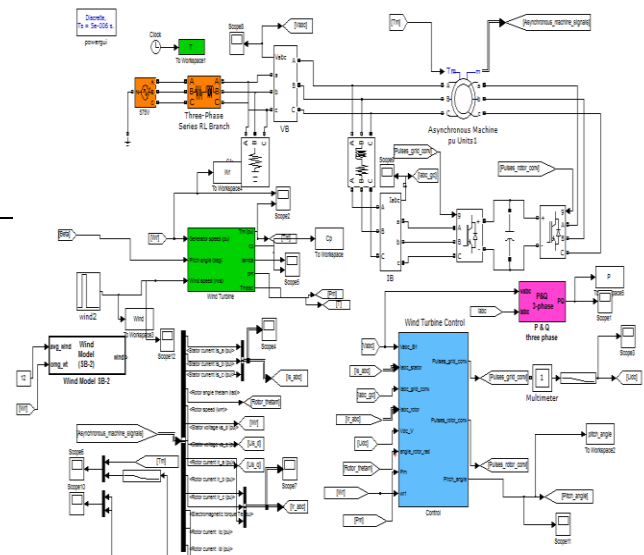


Fig..22.Simulation scheme of a 1.5 MW doubly-fed induction generator wind turbinegenerator system.

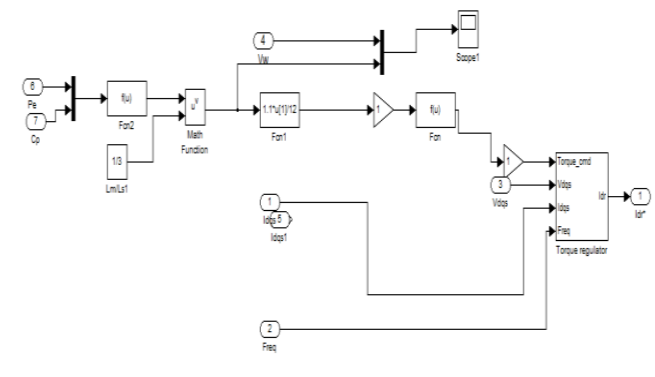


Fig.23 Simulation scheme Control Current